

# Using monkey hand exoskeleton to explore finger passive joint movement response in primary motor cortex

Kai Qian, Luiz Antonio dos Anjos, Jr., Karthikeyan Balasubramanian, Kelsey Stilson, Carrie Balcer, Nicholas G. Hatsopoulos and Derek G. Kamper

**Abstract**— While neurons in primary motor cortex (M1) have been shown to respond to sensory stimuli, exploration of this phenomenon has proven challenging. Accurate and repeatable presentation of sensory inputs is difficult. Here, we describe a novel paradigm to study response to joint motion and fingertip force. We employed a custom exoskeleton to drive index finger metacarpophalangeal joint (MCP) of a macaque to follow sinusoid trajectories at 4 different frequencies (0.2, 0.5, 1, 2 Hz) and 2 movement ranges (68.4, 34.2 degrees). We highlight results of a specific M1 unit that displayed sensitivity to direction (more active during flexion than extension), frequency (greater firing rate at higher frequencies), and movement amplitude (higher rate at larger amplitude). Joint movement trajectories were accurately reconstructed from this single unit with mean  $R^2 = 0.64 \pm 0.13$ . The exoskeleton holds promise for examination of sensory feedback. In addition, it can be used as an external device controlled by a brain-machine interface (BMI) system. The proprioceptive related units in M1 may contribute to improving BMI control performance.

## I. INTRODUCTION

“One can only control what one senses.” [1]. This statement is true for biological as well as robotic control systems. Animals have exquisite sensory feedback, enabling them to perform precision tasks in a variety of conditions, even in the absence of visual feedback. Sensory afferent inputs conveying kinesthetic or proprioceptive information, for example, are critical to hand dexterity. Loss of this feedback, such as through deafferentation, profoundly affects movement accuracy and adaptability [2].

As important as the sensory cells in the periphery are to sensory feedback, processing in the central nervous system is equally critical. Traditionally, it was thought that somatosensory cortex (S1) was primarily responsible for sensory perception and analysis. Cells in somatosensory cortex have shown active response to joint movement or to different gesture configurations, and to tactile inputs [3, 4]. In contrast, primary motor cortex (M1), has been considered an active movement execution center with efferent neurons. Yet, a number of cells in M1 also respond to active and passive joint movements and cutaneous inputs [5-7]. After ablation of

S1, monkeys can still detect passive movements [8], suggesting that cells in other areas, such as M1, may contribute to the perception of passive movement.

Previous research on afferent responses in M1, however, was performed by manually manipulating a joint or applying cutaneous stimuli [5, 6]. The state of the animal could not be rigidly controlled. In this study, we utilized techniques to ensure that passive responses to joint movement and fingertip force development were investigated in the index finger of a rhesus macaque monkey. Using a novel, actuated hand

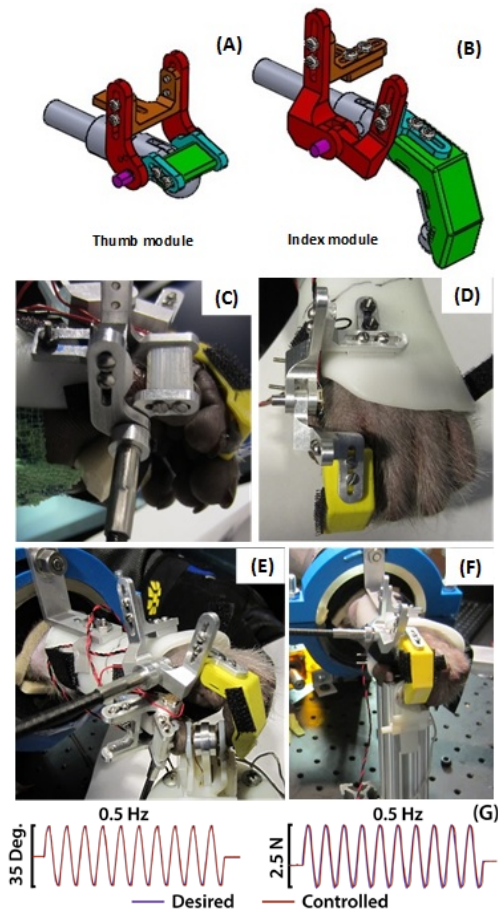


**Figure 1.** Monkey hand exoskeleton. (A) Thumb module, rotation shaft aligned with IP joint, marked pink. (B) Index module, rotation shaft aligned with MCP joint in pink color. (C) Thumb module was mounted on a hand splint over proximal finger segment. (D) Index module was mounted on a hand splint at the dorsal side. (E) Full exoskeleton setup with 4 mm diameter flexible shaft connected to the driving shaft. Pinch force sensor embedded with two load cells was located midway between index finger and thumb. (F.) Index finger passive movement setup for this study. Pinch sensor was mounted underneath the hand within the flexion range of the index finger. (G) Control trajectories of 0.5 Hz joint movement (left), and 0.5 Hz tactile force (right) of the index module.

\*Research supported by NIH NCATS UL1TR000430 awarded to DGK, NIH R01 NS045853 from the NINDS awarded to NGH

K. Qian, L. Anjos are with Department of Biomedical Engineering, Illinois Institute of Technology, Chicago, IL, 60616, USA (phone: 312-567-6897; e-mail: kqian@hawk.iit.edu).

K. Balasubramanian, K. Stilson, C. Balcer, N. Hatsopoulos, are with Department of Organismal Biology and Anatomy at the University of Chicago, Chicago, IL 60637 USA.

D. Kamper is with the Joint Department of Biomedical Engineering at North Carolina State University and the University of North Carolina at Chapel Hill, Raleigh, NC 27606 USA.

exoskeleton, we moved the metacarpophalangeal (MCP) joint at 4 different frequencies over 2 movement ranges. We also generated fingertip force of 3 frequencies and 3 levels, all while simultaneously recording from M1 with a cortical electrode array. Index finger and thumb muscle activation were blocked by injection of botulinum toxin. We hypothesized that some M1 neurons would respond to the joint angle movement while others would respond to fingertip force. We reported results of joint movement here, and detailed results of fingertip force will be reported in later paper.

## II. METHODS

### A. Monkey Hand Exoskeleton

A two degree-of-freedom (DOF) hand exoskeleton was developed to examine pinch sensorimotor control in the rhesus monkey. The exoskeleton had an index finger module, controlling flexion/extension of the metacarpophalangeal joint, and a thumb module, controlling flexion/extension of the interphalangeal (IP) joint. Both modules were anchored on a hand splint, fabricated from Thermoplast, with 3D adjustment (index) and 2D adjustment (thumb) mechanism to align the exoskeleton rotational axes to the corresponding anatomical axes (Fig. 1). All of the remaining joints of the index finger and thumb were fixed at angles appropriate for palmar pinch with a plastic splint (Fig. 1). The splint was secured to the forearm and hand with Velcro straps. The splints were further secured by attaching them directly to the fingernail and thumbnail with cyanoacrylate adhesive (super-glue; Fig. 1). The adhesive was removed after the experiment by rinsing with acetone.

Two servo motors (AKM series, Kollmorgen, Radford, VA) were coupled to the two exoskeleton DOF by flexible shafts to control rotation at the MCP and IP joints. Mini rotary position sensors (linearity rated as 2%, SVM4A, Murata, Kyoto, Japan) were mounted on the rotating shafts of the thumb and finger modules to measure actual joint movement, used in the controller.

The monkey digits made contact with a custom fixture to measure pinch force. Two subminiature load cells (ML13, 1Kg, Honeywell, Columbus, OH) embedded in the fixture measured the index and thumb isometric grip force individually (Fig. 1). Joint position or force was controlled by separate PI controllers running at 1 kHz. The controllers were programmed within Matlab Simulink Real-time and ran on a target computer communicating with a host computer running a customized Matlab GUI. This GUI enabled parameter selection for the experiment.

### B. Subject

One adult male rhesus macaque participated in the experiment. The animal was first trained to sit in a primate chair with forearm restrained by a well-padded arm rest mounted on a table in front of him. A padded elbow block prevented elbow rotation. Then, 21 days before this experiment, botulinum toxin (BTX) was injected into selected muscles of the index finger and thumb to block muscle activation. The BTX effects were evaluated by a fruit gathering task every day. The monkey exhibited profound weakness in the index finger and thumb after the injection; motor ability gradually recovered after 4 weeks. The monkey had previously been chronically implanted with a

100-electrode microelectrode array (Blackrock Microsystems, Inc., Salt Lake City, UT) in M1 contralateral to the hand used for the task. All of the surgical and behavioral procedures were approved by the University of Chicago Institutional Animal Care and Use Committee and conform to the principles outlined in the Guide for the Care and Use of Laboratory Animals

### C. Experiment Procedures

For this experiment, only the index module was used. Joint limits within the exoskeleton were first determined by manually moving the index finger MCP joint with the motor turned off. Two motion ranges were used: 90% and 45% of the full flexion-extension interval, centered in the middle of the range. The exoskeleton was then activated to impose movement of the MCP joint. From the initial center position, the MCP joint was moved in sinusoidal trajectories of one of four frequencies (0.2, 0.5, 1, 2 Hz). All four frequencies were tested at both amplitudes, 90% of full range and 45% of full range. Each sinusoidal trajectory lasted 20s. A 10s rest period was allotted between each movement trajectory. During this rest period, the exoskeleton held the joint steadily in the central posture. Three movement trials were performed for each of the 8 conditions (Fig. 3).

After the joint movement session, an additional tactile force session was conducted. Here, the index fingertip was driven against the force sensor to generate sinusoidal tactile forces with frequencies of 0.2, 0.5, and 1 Hz and amplitudes of 0.5, 1, and 2 N. During the entire experiment, the monkey's view of the exoskeleton device and his hand was blocked by a foam sheet.

### D. Neural data analysis

Spike waveforms were sorted off-line and analyzed in MATLAB. For each unit identified, its spike train was binned within a 1-ms window. Continuous firing rate estimation was obtained by convolving the spike train with a Gaussian kernel [9]. The standard deviation of the kernel was set to 30 ms. For

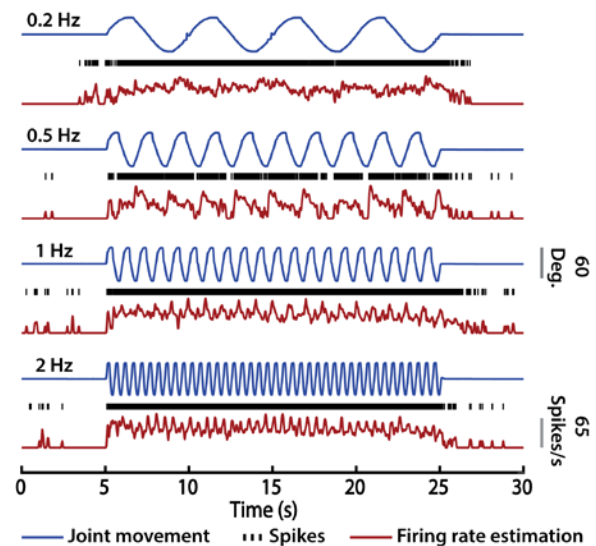


**Figure 2.** Firing rate of a M1 unit response to passive joint movements. Each trial consisted of 20 s movement period and 10 s rest (steady) period. Movement, spikes, firing rate estimation were aligned with time. Firing rate estimation trajectories (red) showed similar patterns as joint movements (blue) as joint movement frequency varied.

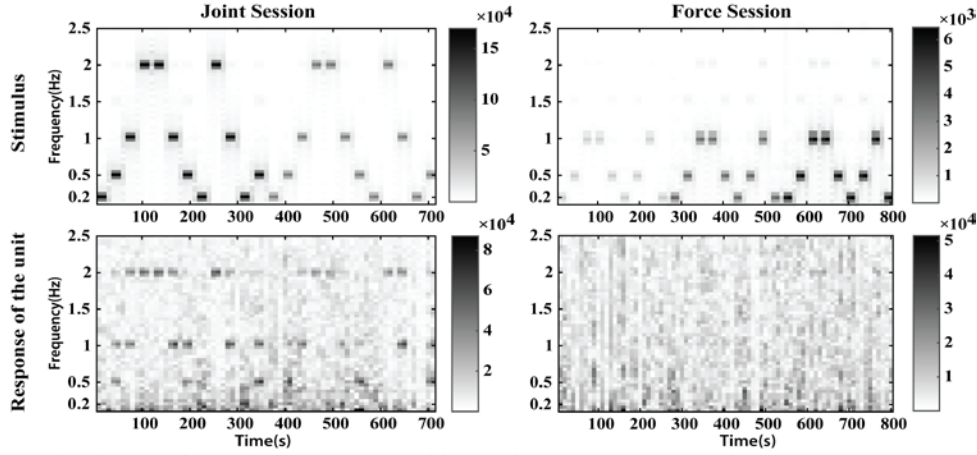


**Figure 3.** Time-frequency plot of the stimulus and firing rate response of the sample M1 unit. Frequency and movement range variations for each trial can be identified from the joint stimulus session graph (top left). Frequency and force level variations for each trail are also shown in the force stimulus session plot (top right). For the joint session, the M1 unit firing rate response showed frequency components similar to stimulus, albeit, with additional harmonic frequencies. For the tactile force session, the M1 unit firing rate response did not exhibit similar frequency components to that of the stimulus.

clarification, firing rate estimation refers to this continuous firing rate trajectory in the rest of the paper. Average firing rate refers to spike counts divided by data segment time. Time-frequency analysis was performed on the entire firing rate estimation trajectory and stimulus trajectory to examine if the firing rate response to the stimulus exhibited similar time-varying frequency features. The spectrogram was calculated using a Hamming window, with window length of 20,000 data points, 50% overlap, without zero padding, and a sampling rate 1 kHz. Frequency components below 0.05Hz were removed before generating the time-frequency plot in order to reduce the large DC component influence so as to obtain better color contrast. For flexion and extension analysis, data were split into segments according to movement peaks. For each trial, data from the first complete flexion segment to the last complete extension segment were used (420 segments in total, 210 each). Two incomplete flexion segments and the first extension segment of each trial were excluded from the paired analysis. Average firing rate was used for statistical analysis.

Joint movement stimuli were also reconstructed from binned spike data using a causal Wiener Filter [10, 11].

$$\hat{y}_i = \sum_{j=0}^M h_j x_{i-j} + \bar{y} \quad (1)$$

$h_j$  is filter coefficient, filter length is  $M+1$ ,  $\hat{y}_i$  is the stimulus estimate at sample index  $i$ ,  $x$  is the binned spike centered with zero mean,  $\bar{y}$  is mean of stimulus of that trial, and  $h_j$  is determined by the Wiener-Hopf equations.  $M$  was chosen to correspond to the period of the sinusoid (e.g.  $M = 500$  for 2 Hz movement, sampling rate 1 kHz). Reconstruction was done trial by trial. The first second and last second of the trial (transition periods) were removed.

### III. RESULTS

The large and small movement ranges used for the experiment were 68.4 and 34.2 degrees, respectively. For clarifications, movement in the flexion direction corresponded to an increase in joint angle. In this experiment, we were able to isolate 46 units. A total of 16 units responded to joint

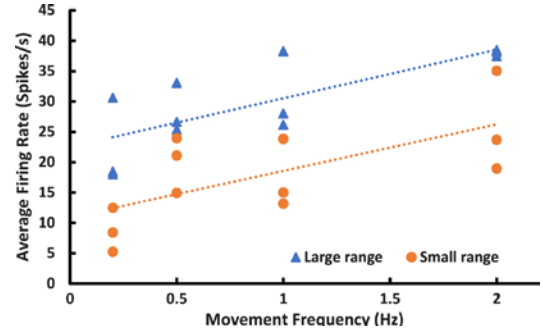


**Figure 4.** Average firing rates of the M1 unit across joint movement frequencies under two movement ranges. Each point represented one trial (three trials per condition). Both ranges showed an increasing trend.

movements: 5 were inhibited while 11 were excited during joint movement. Another two units modulated activity in accordance with tactile force stimuli. One unit showed response to both joint angle and fingertip force, based on relevant peaks in power spectral density graph.

We picked a sample unit for detailed analysis. Its firing rate varied with joint state (Fig. 2). The large peaks in firing rate trajectories showed similar frequencies as the movement stimulus. This frequency variation was also revealed in the time-frequency plot (Fig. 3). Firing rate estimation showed temporal and frequency patterns similar to the stimuli across the whole experiment. There was no similar pattern found for the tactile force experiment. Thus, the joint movement response reported for this unit likely did not arise from cutaneous input resulting from the interaction between the finger and exoskeleton, but rather from movement of the joint.

Joint movement information can be assessed from firing rate time-frequency plots (Fig. 3). Excluding the harmonic components, the time-frequency plots for the unit and the stimulus were remarkably similar. In the firing rate plot, the identified frequency components contained greater power (darker) at larger frequencies and at the bigger movement range. The unit's average firing rate showed a trend to increase with greater movement frequency and was greater for larger movement amplitudes (Fig. 4). A magnified view of movement trajectory and firing rate estimation showed that



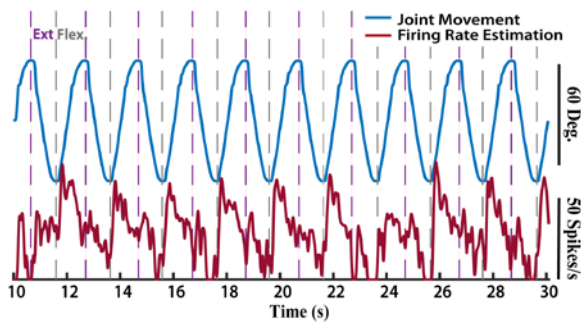


**Figure 5.** Magnified view of firing rate estimation vs. movement. The unit tended to firing more during flexion movement (upward direction).

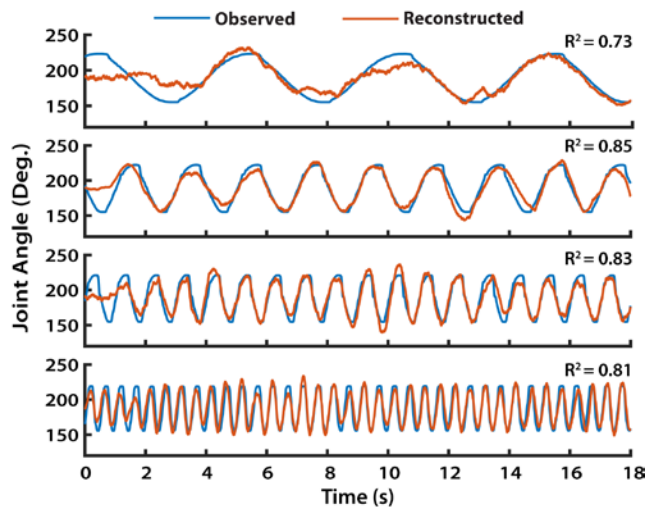


**Figure 6.** Joint movement trajectories reconstructed from the single unit spike train. Reconstructions were done on individual trials.

the unit appeared to fire more strongly during the flexion part of the movement (Fig. 5). Results of a paired t-test revealed that there was a directional dependence for firing rate ( $t = 25.40$ ,  $df = 419$ ,  $p\text{-value} < 0.0001$ ). The unit exhibited a firing rate that was higher by 10.07 spikes/s during flexion than during extension (95% confidence interval: 9.29 - 10.84).

Joint motion could be reconstructed accurately from even a single unit. Across frequencies and movement ranges the average fit  $\pm$  standard deviation of the reconstructed trajectory was  $R^2 = 0.64 \pm 0.13$ . For individual trials, this could be as high as  $R^2 = 0.85$  (Fig. 6).

#### IV. DISCUSSION

Of the 46 units from which we recorded in M1, over 40% displayed firing patterns associated with sensory input to the index finger. Other units may have also exhibited sensory responses, but for other digits. In agreement with previous studies, the majority of the responsive units contained information related to joint movement rather than force [5-7]. Furthermore, preferential firing was observed not only for sensory modality (movement vs. force), but also for movement direction (flexion vs. extension). For example, the sample unit reported here responded preferentially to flexion movements. Other units were inhibited by movement, or fired more during extension. Reconstruction, with a fit of  $R^2 > 0.8$ , could be achieved from even a single unit.

Muscle spindles, cutaneous receptors and joint receptors

may all contribute to such passive movement responses. Identification of the exact source of sensory input to M1 is complicated by the degree of convergence of afferent information in M1, especially in comparison with somatosensory cortex. BTX was injected into finger and thumb muscles to block muscle activation. One concern is the potential effect of BTX on intrafusal fibers which influence the gain on muscle spindles. The influence of BTX on intrafusal muscles is, however, still unresolved, as limited animal and human data are available, and conflicting observations exist [12]. The hand exoskeleton used in this study can apply more controlled and complex joint movement stimulus or generate different tactile force patterns at the finger and thumb tip. The thumb module can be driven independently from the index finger module to permit exploration of neural responses to uncoupled as well as coordinated, joint movements. This new device may further the investigation of the passive movement response in M1 and its role in motor control. Additionally, the exoskeleton can also be used as an external device controlled by a BMI system. As units in M1 were found to contain rich information about passive joint movements or tactile force input, these units might be incorporated into a BMI decoder or contribute indirectly through circuits in the cortex to allow natural proprioceptive sensory feedback to be included in BMI systems. Individuals with motor impairment but with largely intact sensory systems (e.g., individuals with amyotrophic lateral sclerosis, muscular dystrophy, and incomplete spinal cord injury), may benefit from BMI systems incorporating exoskeletons rather than external robots.

#### REFERENCES

- [1] D. I. McCloskey and A. Prochazka, "The role of sensory information in the guidance of voluntary movement: reflections on a symposium held at the 22nd annual meeting of the Society for Neuroscience," *Somatosensory & Motor Research*, vol. 11, pp. 69-76, 1994.
- [2] A. Prochazka, "Proprioceptive feedback and movement regulation," *Comprehensive Physiology*, 2010.
- [3] R. M. Costanzo and E. P. Gardner, "Multiple-joint neurons in somatosensory cortex of awake monkeys," *Brain research*, vol. 214, pp. 321-333, 1981.
- [4] R. M. Costanzo and E. P. Gardner, "A quantitative analysis of responses of direction-sensitive neurons in somatosensory cortex of awake monkeys," *Journal of Neurophysiology*, vol. 43, pp. 1319-1341, 1980.
- [5] I. Rosen and H. Asanuma, "Peripheral afferent inputs to the forelimb area of the monkey motor cortex: input-output relations," *Experimental brain research*, vol. 14, pp. 257-273, 1972.
- [6] R. N. Lemon and R. Porter, "Afferent input to movement-related precentral neurones in conscious monkeys," *Proceedings of the Royal Society of London B: Biological Sciences*, vol. 194, pp. 313-339, 1976.
- [7] E. Fetz, D. Finocchio, M. Baker, and M. Soso, "Sensory and motor responses of precentral cortex cells during comparable passive and active joint movements," *Journal of Neurophysiology*, vol. 43, pp. 1070-1089, 1980.
- [8] L. Kruger and P. Porter, "A behavioral study of the functions of the rolandic cortex in the monkey," *Journal of Comparative Neurology*, vol. 109, pp. 439-469, 1958.
- [9] P. Dayan and L. F. Abbott, *Theoretical neuroscience* vol. 806: Cambridge, MA: MIT Press, 2001.
- [10] W. Bialek and F. Rieke, "Reading a Neural Code," *Science*, vol. 252, p. 1854, 1991.
- [11] R. Wessel, C. Koch, and F. Gabbiani, "Coding of time-varying electric field amplitude modulations in a wave-type electric fish," *Journal of Neurophysiology*, vol. 75, pp. 2280-2293, 1996.
- [12] J. M. Gracies, "Physiological effects of botulinum toxin in spasticity," *Movement Disorders*, vol. 19, 2004.